NIH Public Access
Author Manuscript
J Chromatogr A. Author manuscript; available in PMC 2015 November 07.

Published in final edited form as:
J Chromatogr A. 2014 November 7; 1367: 154–160. doi:10.1016/j.chroma.2014.09.040.

Optimization of A Microfluidic Electrophoretic Immunoassay Using a Peltier Cooler

Nikita Mukhitov, **Lian Yi**, **Adrian M. Schrell**, and **Michael G. Roper***
Department of Chemistry and Biochemistry, Florida State University, 95 Chieftain Way, Tallahassee, FL 32306

Abstract

Successful analysis of electrophoretic affinity assays depends strongly on the preservation of the affinity complex during separations. Elevated separation temperatures due to Joule heating promotes complex dissociation leading to a reduction in sensitivity. Affinity assays performed in glass microfluidic devices may be especially prone to this problem due to poor heat dissipation due to the low thermal conductivity of glass and the large amount of bulk material surrounding separation channels. To address this limitation, a method to cool a glass microfluidic chip for performing an affinity assay for insulin was achieved by a Peltier cooler localized over the separation channel. The Peltier cooler allowed for rapid stabilization of temperatures, with 21 °C the lowest temperature that was possible to use without producing detrimental thermal gradients throughout the device. The introduction of cooling improved the preservation of the affinity complex, with even passive cooling of the separation channel improving the amount of complex observed by 2-fold. Additionally, the capability to thermostabilize the separation channel allowed for utilization of higher separation voltages than what was possible without temperature control. Kinetic CE analysis was utilized as a diagnostic of the affinity assay and indicated that optimal conditions were at the highest separation voltage, 6 kV, and the lowest separation temperature, 21 °C, leading to 3.4% dissociation of the complex peak during the separation. These optimum conditions were used to generate a calibration curve and produced 1 nM limits of detection, representing a 10-fold improvement over non-thermostated conditions. This methodology of cooling glass microfluidic devices for performing robust and high sensitivity affinity assays on microfluidic systems should be amenable in a number of applications.

Keywords

Affinity assay; temperature control; thermoelectric; insulin; lab-on-a-chip

© 2014 Elsevier B.V. All rights reserved.

*Address Correspondence to: Dr. Michael G. Roper, Department of Chemistry and Biochemistry, Florida State University, 95 Chieftain Way, Dittmer Building, Tallahassee, FL 32306, Ph 850-644-1846, Fx 850-644-8281, roper@chem.fsu.edu.

Publisher's Disclaimer: This is a PDF file of an unedited manuscript that has been accepted for publication. As a service to our customers we are providing this early version of the manuscript. The manuscript will undergo copyediting, typesetting, and review of the resulting proof before it is published in its final citable form. Please note that during the production process errors may be discovered which could affect the content, and all legal disclaimers that apply to the journal pertain.

NIH-PA Author Manuscript
NIH-PA Author Manuscript
NIH-PA Author Manuscript

NIH-PA Author Manuscript
NIH-PA Author Manuscript
NIH-PA Author Manuscript

1. Introduction

Capillary electrophoresis (CE) can be used for rapid separations, and is frequently used to analyze non-covalent affinity complexes formed in affinity CE (ACE). There are many forms of ACE, with a common theme being the use of a binding interaction to quantify an analyte of interest. Common binding agents employed are receptors, antibodies, enzymes, and aptamers [1–4], which allow quantitation of analytes in complex samples [5–10]. Additionally, ACE can also be applied for the determination of binding and kinetic information of the affinity interactions, as well as conformational changes [11–13].

The effectiveness of ACE assays depends strongly on the ability to separate the affinity complex from the free species, or a reference marker. In turn, a requirement that arises for successful execution is the maintenance and preservation of the affinity complex during the separation [14–16]. Once the separation is initiated, a non-equilibrium environment is introduced and the complex species begins to dissociate. There are two means to minimize dissociation of the non-covalently bound complex species: minimize the time spent during the separation and reduce the dissociation rate constant (k_{off}). To minimize separation times, a combination of short separation distances with high electric fields can be used, although some work has demonstrated detrimental effects of high electric fields on affinity complexes [17–19]. To minimize k_{off}, the temperature of the separation can be reduced [17]. However, heating produced as a result of increased separation voltages, which can be up to 10 – 60 °C above ambient [20], can greatly affect the affinity complex [21–23]. To mitigate Joule heating, methods of thermal control and cooling during separation have been developed and are often utilized [24–25].

Microfluidic chips have also been prevalent in the use of affinity assays, taking advantage of the integration of sample handling steps with the separation [9,10,26]. Although the separation times are typically shorter than those encountered in capillary systems, microfluidic separations are also confounded by Joule heating, and the thermal mass of microfluidic systems are often higher than those in capillaries. For high efficiency separations, glass is frequently the material of choice for microfluidic separation systems; however, due to the low thermal conductivity of this material (~1 $Wm^{-1}K^{-1}$) any heat generated during operation will not be dissipated rapidly. Additionally, unlike the thin cylindrical capillaries that are used in CE which are exposed on all sides to coolant or air, microfluidic separation channels are often surrounded by the large thermal mass of the device itself. An example of the insulating power of glass was shown in a previous report that compared heating and cooling rates in glass microfluidic devices with and without bulk glass surrounding the microfluidic channels. Cooling and heating rates increased 3.6- and 7.5-fold, respectively, in the glass microfluidic devices without the bulk glass around the channel [27].

Due to the insulating properties of glass, the high temperatures that can occur during Joule heating, and the sensitivity of affinity assays to temperatures, we set out to develop a temperature control system for use in microfluidic affinity assays. A manifold was developed to house two temperature control elements, one for cooling the separation channel and the other for maintaining a stable temperature over the remaining portion of the device.

NIH-PA Author Manuscript

NIH-PA Author Manuscript

NIH-PA Author Manuscript

The effects of cooling were evaluated by determining the preservation of the affinity complex of a competitive immunoassay for insulin. It was found that the addition of a cooler was advantageous for affinity complex preservation leading to ~10-fold decrease in the limit of detection compared to an assay performed without temperature control. In addition, the methodology was relatively simple to implement and would be advantageous to a number of microfluidic affinity assays.

2. Materials and Methods

2.1 Chemicals and Reagents

Dibasic and monobasic potassium phosphate, sodium carbonate and bicarbonate, bovine insulin, and Tween-20 were purchased from Sigma Aldrich (Saint Louis, MO). Ethylenediamine tetraacetic acid (EDTA), bovine serum albumin (BSA), sodium hydroxide, and ammonium hydroxide were obtained from EMD Chemicals (San Diego, CA). Nitric acid, hydrofluoric acid, and hydrogen peroxide were obtained from Macron Fine Chemicals, and sulfuric acid was from J.T. Baker (Center Valley, PA). For all solutions and sample preparation, ultrapure deionized water was used (NANOpure Diamond TM deionization system, Barnstead International, Inc., Dubuque, IA).

The following reagents were utilized for the insulin immunoassay. Monoclonal antibody (Ab) for the C-terminal of human insulin was obtained from Meridian Life Science, Inc. (Torrance, CA). For production of Cy5-labeled insulin (Ins*) Cy5 monofunctional N-hydroxysuccinimide ester was obtained from GE Healthcare Bio-Sciences (Piscataway, NJ). The methodology for labeling bovine insulin has been described previously [7] and was performed according to the manufacturer's guidelines.

2.2 Fabrication of Microfluidic Chips

The methodology for the fabrication has been described in previous work [10]. Briefly, borofloat photoresist wafers (Telic Co., Valencia, CA) with a layer of AZ1500 positive photoresist on a chrome layer were exposed to 18 mW cm^{-1} collimated UV radiation (OAI, San Jose, CA) for 15 s through a patterned photomask. The exposed photoresist was removed with AZ 400K Developer (AZ Electronic Materials Corp., Sommerville, NJ). Subsequently, the bottom chrome layer was developed with a chrome etchant solution (CR-7S, Cyantek Corp., Freemont, CA). The exposed glass was then etched in a 5:1:3 (v:v:v) mixture of H_2O:HNO_3:HF to a 7 μm depth and 15 μm width. The dimensions of the channels were verified using a P-15 Stylus Profilometer (KLA-Tencor, Milpitas, CA). Fluid access holes were drilled with a 500 μm diamond-tipped drill bit after which the remaining photoresist and chrome were removed. These pieces of glass, and blank glass slides, were cleaned for 30 minutes in a 3:1 (v:v) solution of H_2SO_4:H_2O_2 and subsequently a 5:1:1 (v:v) solution of H_2O:NH_4OH:H_2O_2 heated to 60 °C. Finally, the cleaned slides were bonded to the blank glass at 640 °C for 8 hours.

2.3 Temperature Control

A manifold to hold the microfluidic device and temperature controllers was fabricated in-house from two polycarbonate plates. The bottom plate functioned as the support, and the

NIH-PA Author Manuscript

NIH-PA Author Manuscript

NIH-PA Author Manuscript

top housed reservoirs that were milled into the polycarbonate block. Screws were used to clamp the polycarbonate plates around the microfluidic device with o-rings used to form liquid-tight seals for the reagent and separation reservoirs.

The Peltier device (7.0 × 15.0 mm, 11.3 W, Custom Thermoelectric, Bishopville, MD) was held above the separation channel in the top piece of polycarbonate. The device was operated using software from the manufacturer with an Accuthermo FTC-100D controller (Freemont, CA) that used the temperature from a J-type thermocouple (SA1-J, Omega Engineering Inc., Stamford, CT) as an input. The thermocouple was attached to the bottom of the microfluidic device directly below the separation channel. Unless otherwise noted, any temperature expressed throughout this report was the temperature that this thermocouple was reading. The Peltier was attached to the microfluidic device with Arctic Silver 5 thermal compound (Visalia, CA) and a heat sink was attached to the hot side of the Peltier using the same thermal compound. Air was blown over the heat sink at a rate of ~15 L/min using a Welch 2546-B air pump (Niles, IL).

To maintain ambient temperature throughout the remaining portion of the microfluidic device, two thermofoil heaters (Omega Engineering) were combined in parallel and placed under the microfluidic device, upstream of the separation channel. The complementary thermocouple was placed on the top of the microfluidic device and the temperature from this thermocouple was input into a controller (CNi32, Omega Engineering) to maintain the set temperature.

2.4 Detection and Microfluidic Chip Operation

For all experiments, the assembled manifold with microfluidic device was attached to the stage of a Nikon Eclipse TS-100F inverted fluorescence microscope (Nikon Instruments Inc., Melville, NY). Laser-induced fluorescence detection was performed using a 635 nm laser (Aixiz, Houston, TX). The laser was directed into the microscope with a 2 m fiber bundle and collimated using a collimating lens (CeramOptec, East Longmeadow, NY). The collimated light was then directed to a 646 nm dichroic (Semrock, Rochester, NY) and projected to a 40 X, 0.6 NA objective (Nikon Instruments Inc.) where it was focused through a hole in the bottom of the manifold into the microfluidic device. Emission light was collected through the same objective and passed through the dichroic mirror, a 685 nm bandpass filter (Semrock), a spatial filter, and then made incident on a photomultiplier tube (PMT). The spatial filter and PMT were housed in a single unit from Photon Technology International Inc. (Birmingham, NJ). Instrument control and data collection were performed by a custom program written in LabView.

The microfluidic design consisted of a reservoir at the top of the device connected to a single sample delivery channel 4 cm in length. The device design was similar to one previously described [10]. A gated injection scheme was utilized with a 1 s sample injection and a 24 s separation [28]. Injections were performed in serial, with an injection occurring after the end of the previous separation. The sample reservoir was connected to ground and the separation voltage was applied to the waste reservoir.

NIH-PA Author Manuscript

NIH-PA Author Manuscript

NIH-PA Author Manuscript

Prior to use, the microfluidic device was conditioned for 1 hour in 1M NaOH, followed by water, and experimental buffers for at least 15 minutes each, prior to commencement of experiments. The reservoirs were loaded with 80 μL of the appropriate solution, sealed with tape, and punctured with Pt electrodes for operation.

2.5 Immunoassay Sample Preparation

Samples were made in 20 mM NaH_2PO_4, 1 mM EDTA, pH 7.4 with 0.1 % (w/v) Tween 20 and 1 mg/mL BSA added. The separation buffer consisted of 20 mM sodium carbonate and 20 mM sodium bicarbonate. For all immunoassay samples, 50 nM Ins* and 50 nM Ab were used with varying concentrations of unlabeled insulin (Ins). The samples were left to equilibrate in the dark at room temperature for 10 minutes prior to placing in the device.

2.6 Data Analysis

The amount of Ins* free (F) and bound (B) to Ab were quantified by peak area using available software [29]. Peak start and finish times were approximated by events that exceeded three times the standard deviation of the baseline. To obtain a calibration curve, the average bound-to-free ratio (B/F) from 5 consecutive electropherograms was evaluated as a function of [Ins] and was fit using a four parameter logistic model [10,14]. The LOD was determined as the concentration of Ins required to induce a change in the B/F greater than three times the standard deviation of the blank. All values throughout the text are reported as an average of 5 consecutive runs with errors reported as +/− 1 standard deviation.

3. Results and Discussion

Temperature control has been utilized in a number of microfluidic applications, including temperature gradient focusing [30,31], isoelectric focusing [32], free flow electrophoresis [33], and zone electrophoresis [34]. Temperature control on microfluidic devices has been performed in a variety of manners [35], from copper blocks [30,31] to Peltier elements [33] to channels carrying temperature-controlling fluids integrated next to features of interest [36]. While much work has gone into implementing temperature control methods for these assays, little has been done on implementing methods for optimization of affinity separations in microfluidic separations even though the affinity complex shows a strong dependence on temperature [21–23]. In this work, active cooling over the separation channel was implemented in an affinity assay for insulin, and it is anticipated that this strategy will be of use to a number of other applications.

3.1 Description of Heating and Cooling Elements

The schematic for the microfluidic device and the placements of the thermofoil (shaded light grey) and Peltier (shaded dark grey) are shown in Figure 1A. Approximately 1.4 cm of the 1.5 cm separation channel was covered by the cooler, allowing the majority of the separation to be performed in the temperature-controlled region while detection was performed at the end of the separation channel, outside the Peltier to reduce scattered laser light. The temperature of the Peltier could be controlled to ± 0.1 °C of the desired temperature. Initial experiments indicated that the Peltier was also lowering the temperatures of the sample and

NIH-PA Author Manuscript

NIH-PA Author Manuscript

NIH-PA Author Manuscript

sample delivery channel. In order to maintain the temperature outside the separation region, a thermofoil heater was used to maintain the sample reservoir and sample delivery channel at approximately room temperature (26 °C) during all experiments. As will be discussed in Section 3.2, regulating the temperature of these areas was important to maintain the equilibrium of the bound and free species prior to separation. All of these components were held in place using a polycarbonate manifold. The manifold, thermofoil and thermocouple, Peltier and its heat sink are shown in Figure 1B. It was found that reproducible placement of the cooler was essential for reproducible separations, necessitating the use of the manifold to maintain the position of the microfluidic device with respect to the position of the heater and cooler.

3.2 Optimization of Temperature at 4.5 kV Separation Voltage

Initial testing of the effect of cooling on the performance of the microchip immunoassay was tested without Ins in the equilibrium mixture. The highest B/F and the variance of this point are critical as it sets the constraints for the sensitivity of the assay. We have used the B/F value at this initial point as a marker of whole assay sensitivity in the past [14].

Ambient temperature of the device was ~26 °C, and without the use of any temperature control, the temperature rapidly increased to ~28 ± 1 °C when a separation voltage of 4.5 kV was applied. This separation voltage was initially evaluated because it was used in our previous studies [10]. The increased temperature was attributed to Joule heating induced by the applied separation voltage. Under these conditions, the B/F ratio was 1.43 ± 0.05 (Figure 2). The microfluidic device was then placed within the manifold containing the Peltier and air was delivered across the heatsink for passive cooling. As a result, the temperature of the separation channel decreased back to ambient (26.0 ± 0.4 °C). This passive thermostating with the heatsink alone produced more than a two-fold improvement of the B/F to 3.53 ± 0.05 (Figure 2). This result emphasizes the necessity of temperature control in affinity assays performed on glass microfluidic devices.

Subsequently, active cooling was applied to further lower the temperature and stabilize the affinity complex. Representative electropherograms during active cooling are shown in Figure 2 at temperatures of 25, 23, 21, 19, and 17 °C. Lower temperatures were not possible due to arcing of the separation voltage, thought to be due to condensation on the device at these lower temperatures. As temperatures decreased below 26 °C, the B/F increased with the highest value found at 21 °C. As the temperature was brought below 21 °C, the B/F began to decrease. Table 1 shows the average B/F at all temperatures tested. Upon the introduction of passive air cooling, or active cooling by the Peltier, the reproducibility of the B/F ratios, as determined by the %RSD, was more than two-fold higher than the non-cooled assay performed at 28 °C.

The initial increase in B/F as the temperature decreased from 26 to 21 °C was due to the stabilization of the complex during the separation. This is evidenced by an increase in the area of the bound complex peak and a decrease in the area between the bound and free peaks where dissociated complex would reside (Supplementary Table 1) [13]. The reduction in the B/F at temperatures below 21 °C was likely due to a shift in equilibrium conditions in the sample delivery channel prior to injection into the separation channel, seen as a decrease in

NIH-PA Author Manuscript

NIH-PA Author Manuscript

NIH-PA Author Manuscript

the area of the bound peak and an increase in the area of the free peak (Supplementary Table 1). This result suggested that the cooling was bleeding into the sample delivery channel, reducing the binding and decreasing the B/F. Although an attempt was made to control the temperature over the sample delivery channel, at temperatures lower than 21 °C in the separation region, a thermal gradient may have developed affecting the equilibrium concentrations of bound and free. Since the bound peak area decreased with cooling past 21 °C, lower temperatures were not investigated during further experiments.

3.3 Optimization of Separation Voltage

The next step towards increasing the sensitivity of this affinity assay was to decrease the separation time. An effort to use a shorter separation channel was attempted, but was unsuccessful due to the constrained positioning of the Peltier cooler with respect to the device geometry. For other applications or in future experiments, it may be possible to change the geometry of the channels to obtain shorter channel lengths. Without the ability to decrease the channel length, the separation voltage was increased to 6 kV to achieve faster separation times. While faster separations are beneficial for ACE, it has been shown that high electric fields, outside of the effects of Joule heating, can also contribute to dissociation of the complex during ACE separations [17,18]. While these effects have only been reported in ACE separations involving DNA aptamers as the binding reagent, a separation voltage of 3 kV was also evaluated for this consideration.

Separations at 3, 4.5, and 6 kV were performed at 26, 25, 23, and 21 °C. The 6 kV separations resulted in decreased migration times while maintaining a satisfactory resolution. We found that 6 kV could be applied without thermal control, producing a B/F of 3.08. However, at this voltage, the temperatures increased above 28 °C and severely limited the reproducibility of the assay. The integration of the cooler was essential to decrease the detrimental effects of Joule heating at this higher voltage. The shorter residence times in the separation channel were beneficial for preservation of the affinity complex as the B/F was larger than those of the 4.5 kV separations at all temperatures tested (Supplementary Data, Table 2), with the highest at 21 °C. At a separation voltage of 3 kV, the B/F also increased with colder temperatures, but were lower than the B/F values at 4.5 and 6 kV (Supplementary Data, Table 2). There was also severe fronting of the bound peak during separations at 3 kV, but the cause of the fronting was not determined. Example electropherograms from 3, 4.5, and 6 kV separation voltages at 21 °C are shown in Figure 3.

3.4 Kinetic Capillary Electrophoresis Analysis

To understand the effects occurring at the various temperatures and separation voltages, we determined the k_{off} values at all conditions tested. Additionally, k_{off} measurements can be used to determine ideal conditions for ACE [15,16]. Re-association of the free species is assumed to be negligible during a separation, shifting the attention to lowering k_{off}. To determine k_{off}, the data obtained at the various separation voltages and temperatures were analyzed as described for non-equilibrium capillary electrophoresis of equilibrium mixtures [13]. Using the k_{off} values, we then calculated the percent complex dissociated during the separation [16]. The values of k_{off} and percent complex dissociation are shown in Figure 4

NIH-PA Author Manuscript

NIH-PA Author Manuscript

NIH-PA Author Manuscript

as a function of temperature. The different separation voltages tested are indicated by the shading and shape of the points as described in the figure legend.

As shown in Figure 4A, cooling the separation channel produced a decrease in k_{off} at all applied separation voltages reducing the percentages of the complex peaks that dissociated (Figure 4B). Colder temperatures had the largest effect on the 4.5 kV separations as the percent k_{off} decreased by 55% and the percent dissociated decreased from 9.6% at 26 °C to 5.1% at 21 °C. At 6 kV, cooling did not have as large of an effect on k_{off} as it did for 4.5 kV separations, but because the separation times were smaller at this voltage, the percent complex that dissociated was lower at all temperatures tested with the lowest of 3.3% at 21 °C. The combination of the lowest k_{off} and fastest separation time explains why the highest B/F was observed at this voltage and temperature.

3.5 Calibration at optimal conditions

A calibration curve using the optimized conditions at 6 kV and 21 °C was performed and shown in Figure 5. The LOD for the assay was 1 nM and was an improvement of ~10-fold over un-optimized conditions performed without temperature control at lower voltages. It may be possible to obtain a lower LOD with the use of higher voltages, although the equilibrium dissociation constant (K_d) of the antibody will ultimately limit the sensitivity of this assay [15]. Using similar concentrations of immunoassay reagents with slightly different buffer compositions, we previously reported an LOD of 20 nM for insulin [10]. A major difference between the assays was that the previous microfluidic device was heated upstream of the separation channel to maintain viability of cells placed on the device and to promote mixing of the immunoassay reagents while no cooling of the separation channel was performed. If the heating spread into the separation region, k_{off} would have been large and produced more dissociation of the complex during the separation, decreasing the sensitivity of the assay.

4. Conclusions

The effect of temperature control on microfluidic immunoassays was demonstrated using an offline immunoassay of insulin. Even passive thermal control through the attachment of a heat sink demonstrated a significant contribution to stabilizing the affinity complex during separations. Subsequent application of active cooling yielded a decrease in the dissociation rate constant accompanied by a substantial improvement in the B/F and a lower LOD. Furthermore, the methodology presented allowed for the utilization of higher separation voltages that, in the absence of cooling, would produce Joule heating detrimental for affinity assays.

Several improvements could be made to the current system. For example, although we attempted to localize the cooling over the separation channel, the observation that the equilibrium shifted at temperatures below 21 °C indicates that a better control over the temperature between the various regions in the microfluidic device is required. It may be that a different channel design would have been more ideal or channels with temperature-controlling fluids could be patterned directly into the device for more accurate control over local temperatures. Additionally, if this device is to be applied in future analysis for

NIH-PA Author Manuscript

NIH-PA Author Manuscript

NIH-PA Author Manuscript

measuring insulin secretion from living cells where heating elements are required [10,22], further control will be required to make sure temperature zones are not compromised by adjacent elements. Nonetheless, the use of Peltier elements for temperature control over separation domains provides an additional tool for microfluidic devices and affinity assays in general.

Supplementary Material

Refer to Web version on PubMed Central for supplementary material.

Acknowledgments

We would like to acknowledge the contribution of the FSU Chemistry and Biochemistry department machine shop and in particular Kevin Kiley for the construction of the microfluidic manifold. This work was supported by a grant from the National Institutes of Health (R01 DK080714).

References

1. Guzman AN, Blanc T, Philips TM. Immunoaffinity capillary electrophoresis as a powerful strategy for the quantification of low abundance biomarkers, drugs and metabolites in biological matrices. Electrophoresis. 2008; 29:3259–3278. [PubMed: 18646282]
2. Mairal T, Ozalp VC, Lozano Sanchez P, Mir M, Katakis I, O'Sullivan CK. Aptamers: molecular tools for analytical applications. Anal Bioanal Chem. 2008; 390:989–1007. [PubMed: 17581746]
3. Moser AC, Willicot CW, Hage DS. Clinical applications of capillary electrophoresis based immunoassays. Electrophoresis. 2014; 35:937–955. [PubMed: 24132682]
4. Shimura K, Karger BK. Affinity probe capillary electrophoresis: analysis of recombinant human growth hormone with a fluorescent labeled antibody fragment. Anal Chem. 1994; 66:9–15. [PubMed: 8116876]
5. Koutny LB, Schmalzing D, Taylor TA, Fuchs M. Microchip electrophoretic immunoassay for serum cortisol. Anal Chem. 1996; 68:18–22. [PubMed: 8779431]
6. Tao L, Aspinwall CA, Kennedy RT. On-line competitive immunoassay based on capillary electrophoresis applied to monitoring insulin secretion from single islets of Langerhans. Electrophoresis. 1998; 19:403–408. [PubMed: 9551792]
7. Guillo C, Truong TM, Roper MG. Simultaneous capillary electrophoresis competitive immunoassay for insuing, glucagon and islet amyloid polypeptide secretion from mouse islet of Langerhans. J Chromatogr A. 2011; 1218:4059–4064. [PubMed: 21620410]
8. Chiem N, Harrison DJ. Microchip-based capillary electrophoresis for immunoassays: analysis of monoclonal antibodies and theophylline. Anal Chem. 1997; 69:373–378. [PubMed: 9030052]
9. Shackman JG, Reid KR, Dugan CE, Kennedy RT. Dynamic monitoring of glucagon secretion from living cells on a microfluidic chip. Anal Bioanal Chem. 2012; 402:2797–2803. [PubMed: 22286080]
10. Lomasney AR, Yi L, Roper MG. Simultaneous monitoring of insulin and islet amyloid polypeptide secretion from islets of Langerhans on a microfluidic device. Anal Chem. 2013; 85:7919–7925. [PubMed: 23848226]
11. Gomez FA, Avila LZ, Chu YH, Whitesides GM. Determination of binding constants of ligands to proteins by affinity capillary electrophoresis - compensation for electroosmotic flow. Anal Chem. 1994; 66:1785–1791. [PubMed: 8030787]
12. Kanoatov M, Cherney LT, Krylov SN. Extracting kinetics from affinity capillary electrophoresis (ACE) data: a new blade for the old tool. Anal Chem. 2014; 86:1298–1305. [PubMed: 24380403]
13. Berezovski M, Drabovich A, Krylova SM, Musheev M, Okhonin V, Petrov A, Krylov SN. Nonequilibrium capillary electrophoresis of equilibrium mixtures: A universal tool for development of aptamers. J Am Chem Soc. 2005; 127:3165–3171. [PubMed: 15740156]

NIH-PA Author Manuscript NIH-PA Author Manuscript NIH-PA Author Manuscript

14. Lomasney AR, Guillo C, Sidebottom AM, Roper MG. Optimization of capillary electrophoresis conditions for a glucagon competitive immunoassay using response surface methodology. Anal Bioanal Chem. 2009; 394:313–319. [PubMed: 19189083]
15. Heegard HHN, Kennedy RT. Antigen-antibody interactions in capillary electrophoresis. J Chromatogr B. 2002; 768:93–103.
16. Østergaard J, Heegaard HHN. Bioanalytical interaction studies executed by preincubation affinity capillary electrophoresis. Electrophoresis. 2006; 27:2590–2608. [PubMed: 16732622]
17. Musheev MU, Filiptsev Y, Okhonin V, Krylov SN. Electric fields destabilizes noncovalent protein-DNA complexes. J Am Chem Soc. 2010; 132:13639–13641. [PubMed: 20831170]
18. Buchanan DD, Jameson EE, Perlette J, Malik A, Kennedy RT. Effect of buffer, electric field, and separation time on detection of aptamer-ligand complexes for affinity probe capillary electrophoresis. Electrophoresis. 2003; 24:1375–1382. [PubMed: 12731022]
19. Shultz NM, Kennedy RT. Rapid immunoassay using capillary electrophoresis with fluorescence detection. Anal Chem. 1993; 65:3161–3165.
20. Ross D, Gaitan M, Locascio LE. Temperature measurement in microfluidic systems using a temperature-dependent fluorescent dye. Anal Chem. 2001; 73:4117–4123. [PubMed: 11569800]
21. Berezovski M, Krylov SN. Using nonequilibrium capillary electrophoresis of equilibrium mixtures for the determination of temperature in capillary electrophoresis. Anal Chem. 2004; 76:7114–7117. [PubMed: 15571367]
22. Roper MG, Shackman JG, Dahlgren GM, Kennedy RT. Microfluidic chip for continuous monitoring of hormone secretion from live cells using an electrophoresis-based immunoassay. Anal Chem. 2003; 75:4711–4717. [PubMed: 14674445]
23. Xuan X, Hu G, Li D. Joule heating effects on separation efficiency in capillary zone electrophoresis with an initial voltage ramp. Electrophoresis. 2006; 27:3171–3180. [PubMed: 16850504]
24. Mayer BX. How to increase precision in capillary electrophoresis. J Chromatogr A. 2001; 907:21–37. [PubMed: 11217027]
25. Ma S, Horvath C. Capillary zone electrophoresis at subzero temperatures III. Operating conditions and separation efficiency. J Chromatogr A. 1998; 825:55–69. [PubMed: 9830711]
26. Cheng SB, Skinner CD, Taylor J, Attiya S, Lee WE, Picelli G, Harrison DJ. Development of a multichannel microfluidic analysis system employing affinity capillary electrophoresis for immunoassay. Anal Chem. 2001; 73:1472–1479. [PubMed: 11321296]
27. Easley CJ, Humphrey ACJ, Landers PJ. Thermal isolation of microchip reaction chambers for rapid non-contact DNA amplification. J Micromech Microeng. 2007; 17:1758–1766.
28. Jacobson SC, Ermakov SV, Ramsey JM. Minimizing the number of voltage sources and fluid reservoirs for electrokinetic valving in microfluidic devices. Anal Chem. 1999; 71:3273–3276. [PubMed: 21662916]
29. Shackman JG, Watson CJ, Kennedy RT. High-throughput automated post-processing of separation data. J Chromatogr A. 2004; 1040:273–282. [PubMed: 15230534]
30. Ross D, Locascio LE. Microfluidic temperature gradient focusing. Anal Chem. 2002; 74:2556–2564. [PubMed: 12069237]
31. Munson MS, Meacham JM, Ross D, Locascio LE. Development of aptamer-based affinity assays using temperature gadient focusing: minimzation of the limit of detection. Electrophoresis. 2008; 29:3456–3465. [PubMed: 18646283]
32. Wen J, Wilker EW, Yaffe MB, Jensen KF. Microfluidic preparative free-flow isoelectric focusing: system optimization for protein complex separation. Anal Chem. 2010; 82:1253–1260. [PubMed: 20092256]
33. Yan J, Guo CG, Liu XP, Kong FX, Shen QY, Yang CZ, Li J, Cao CX, Jin XQ. A simple and highly stable free-flow electrophoresis device with thermoelectric cooling system. J Chromatogr A. 2013; 1321:119–126. [PubMed: 24246174]
34. Mitra I, Marczak SP, Jacobson SC. Microchip electrophoresis at elevated temperatures and high separation field strengths. Electrophoresis. 2014; 35:374–378. [PubMed: 24114979]
35. Miralles V, Huerre A, Malloggi F, Jullien M. A review of heating and temperature control in microfluidic systems: techniques and applications. Diagnostics. 2013; 3:33–67.

NIH-PA Author Manuscript

NIH-PA Author Manuscript

NIH-PA Author Manuscript

36. Guijt RM, Dodge A, van Dedem GW, de Rooij NF, Verpoorte E. Chemical and physical processes for integrated temperature control in microfluidic devices. Lab Chip. 2003; 3:1–4. [PubMed: 15100796]

NIH-PA Author Manuscript

NIH-PA Author Manuscript

NIH-PA Author Manuscript

Highlights

- A Peltier cooler was used to minimize dissociation during an affinity separation
- Separation temperatures tested were 26, 25, 23, and 21 °C
- At low temperatures, high separation voltages were permitted
- Optimum conditions were lowest temperature and highest voltage
- LOD improved by 10-fold using optimum conditions

NIH-PA Author Manuscript
NIH-PA Author Manuscript
NIH-PA Author Manuscript

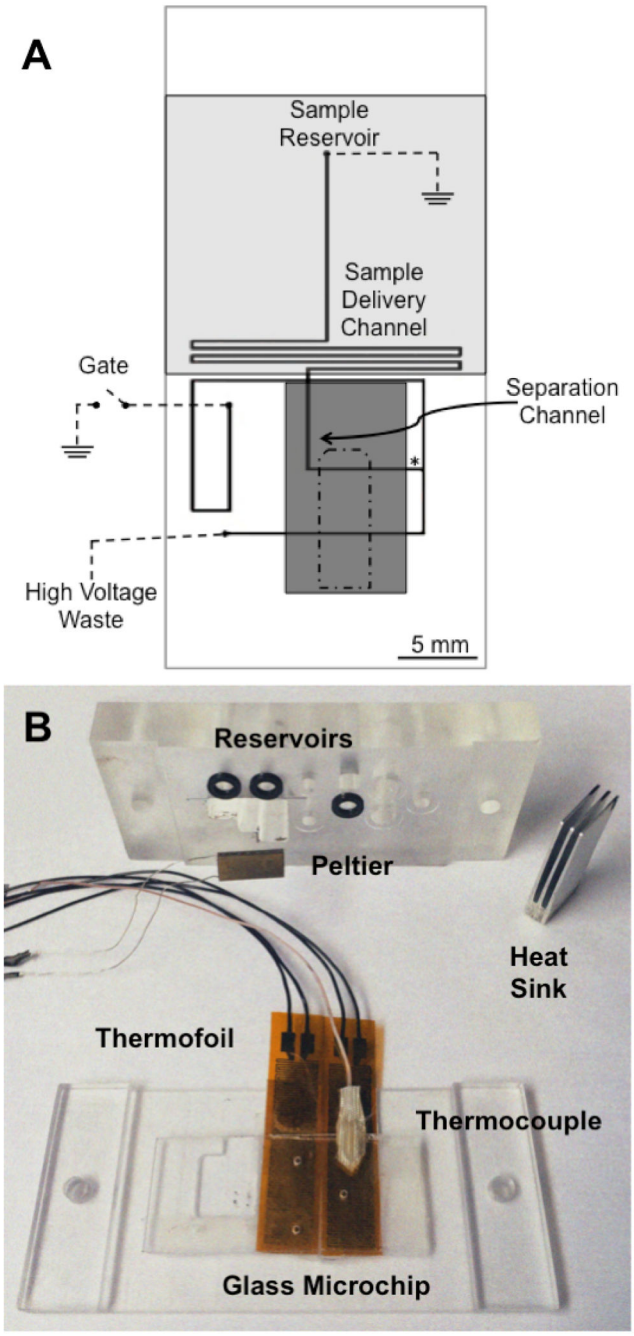

Figure 1. Schematic of microfluidic device indicating positions of the cooler and heater

(A) The design of the microfluidic channels are shown as thick black lines and the electrical connections are shown as dashed lines (---). The reservoirs and channels are labeled on the figure. A thermofoil heater depicted in grey (▫) was localized over the sample reservoir and sample delivery channel. A Peltier cooler was placed over the microfluidic device with its position shown in dark grey (■). The placement of the complementary thermocouple for the Peltier cooler is shown as an outline by a dash dot dash line (-•-). The detection point for the separations is shown as an asterisk (*). **(B)** The manifold used to house the microfluidic

NIH-PA Author Manuscript

NIH-PA Author Manuscript

NIH-PA Author Manuscript

device with the thermofoils, the thermocouple for the thermofoils, the Peltier cooler, and the heat sink are shown. The thermofoils were attached below the device while the Peltier was attached on top. The black o-rings used to make the seals for the fluid reservoirs can also be seen.

NIH-PA Author Manuscript

NIH-PA Author Manuscript

NIH-PA Author Manuscript

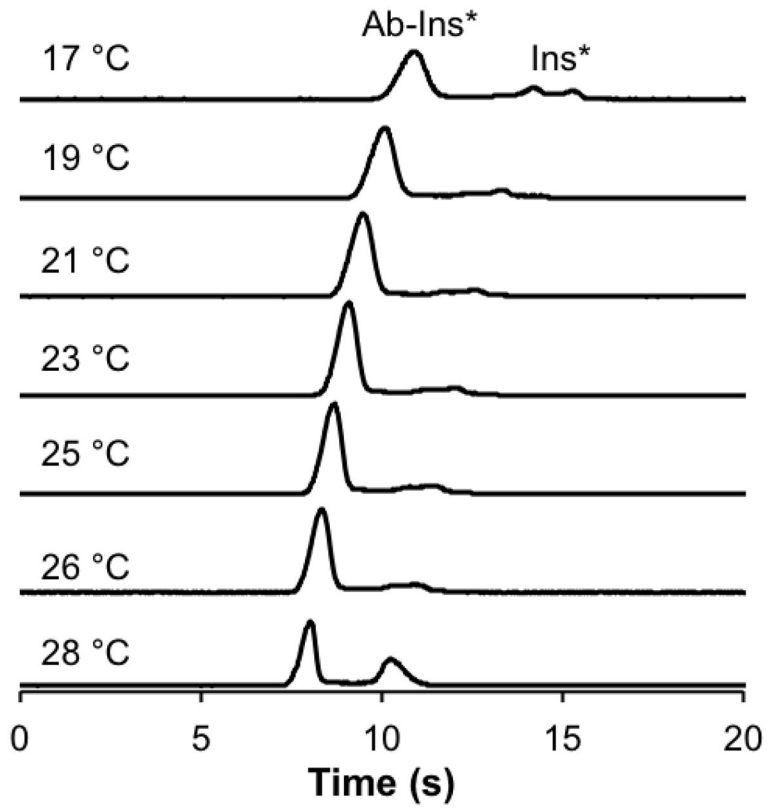

Figure 2. Effect of temperature on the separation of the affinity mixture

50 nM Ins* and 50 nM Ab were used in the affinity assay and 4.5 kV separations performed at the temperatures indicated on the left of the figure. The separation shown at 28 °C was performed without the heat sink on the device and the separation at 26 °C was performed with the Peltier and heat sink on the device and air blowing over the heatsink, but no active cooling was being performed. The traces are offset for clarity but are maintained to scale.

NIH-PA Author Manuscript

NIH-PA Author Manuscript

NIH-PA Author Manuscript

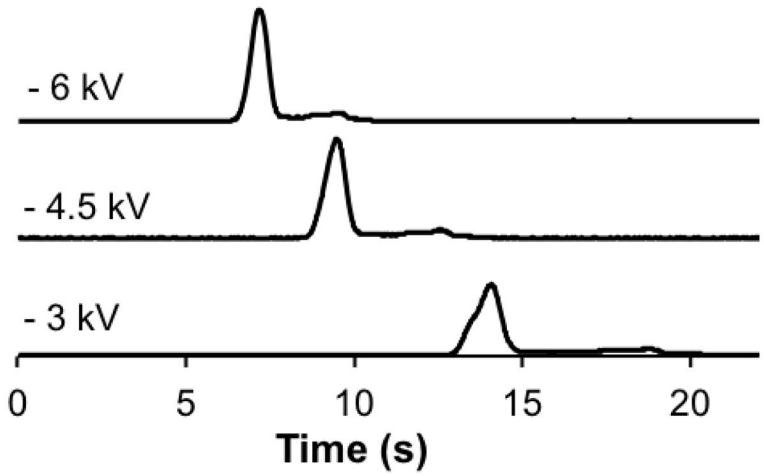

Figure 3. Effect of voltage on the separation of an imunoassay mixture at 21 °C

Three representative electropherograms of the affinity mixture at −3, −4.5, and −6 kV separation voltages are shown. The temperature during these separations was 21 ± 0.1 °C. The traces are offset for clarity and are maintained to scale.

NIH-PA Author Manuscript

NIH-PA Author Manuscript

NIH-PA Author Manuscript

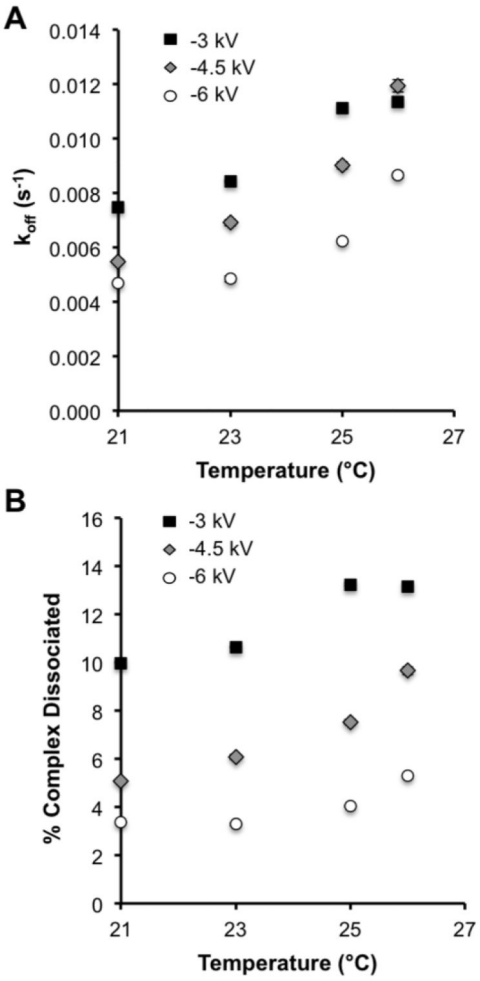

Figure 4. Kinetic effects of separation temperature and voltage

(A) The dissociation rate constant (k_{off}) was determined as described in [12] at the temperatures and voltages shown. The data for −3 kV is shown as the black filled squares (■), for −4.5 kV as grey filled diamonds with a black outline (◆) and for −6 kV as white filled circles with a black outline (○). **(B)** The percent complex dissociated was determined as described in [15]. The symbols are the same as used in part **(A)**.

NIH-PA Author Manuscript

NIH-PA Author Manuscript

NIH-PA Author Manuscript

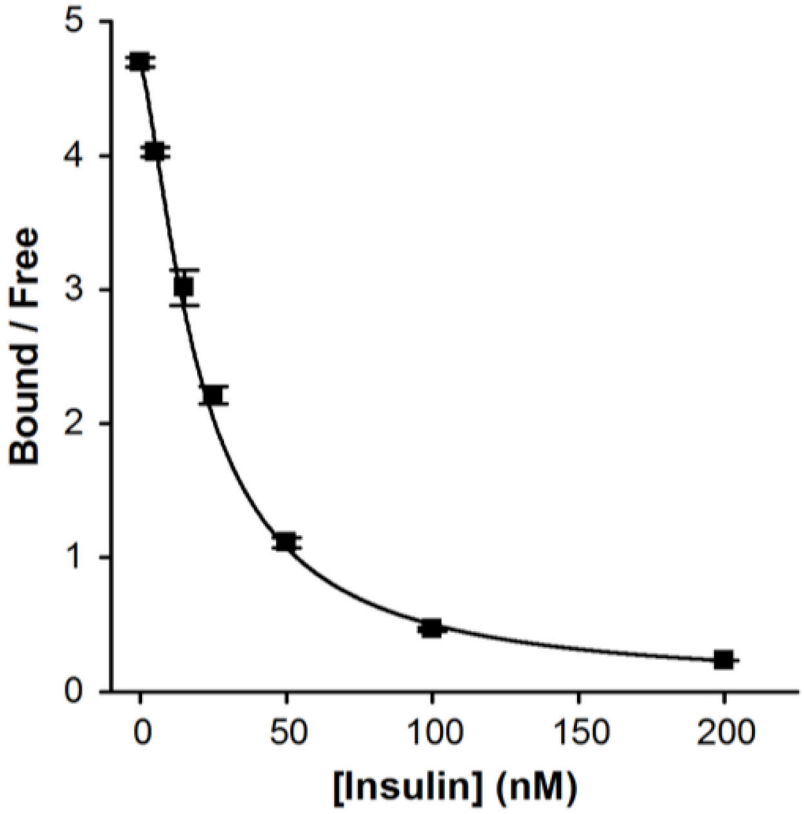

Figure 5. Calibration plot of an insulin immunoassay performed at 21 °C and 6 kV

Bound and free were determined by the areas of the respective peaks. Each point contains an average of 5 runs and error bars represent +/− 1 standard deviation. The data was fit with a four parameter logistic fit (black line) and a 1 nM LOD was calculated.

NIH-PA Author Manuscript

NIH-PA Author Manuscript

NIH-PA Author Manuscript

Table 1

Effect of temperature on the B/F ratio using 4.5 kV separation voltage.

	Temperature (°C)*	B/F	RSD (%)**
No Cooling	28	1.43	3.50
Air Cooling	26	3.53	1.13
Active Cooling	25.0	4.49	1.33
	23.0	5.31	1.50
	21.0	5.76	1.38
	19.0	4.80	0.62
	17.0	2.39	1.25

* The precision of the temperature at 28 °C was ± 1 °C, at 26 °C was ± 0.4 °C, and for others were ± 0.1°C

** The standard deviations reported were determined from 5 consecutive separations